HHS Public Access

Author manuscript

Genes Brain Behav. Author manuscript; available in PMC 2021 November 01.

Published in final edited form as:

Genes Brain Behav. 2020 November ; 19(8): e12690. doi:10.1111/gbb.12690.

Transcriptomic approach predicts a major role for transforming growth factor beta type 1 pathway in L-Dopa-induced dyskinesia in parkinsonian rats

Shetty Ravi Dyavar[1], **Lisa F. Potts**[2], **Goichi Beck**[2], **Bhagya Laxmi Dyavar Shetty**[2], **Benton Lawson**[1], **Anthony T. Podany**[3], **Courtney V. Fletcher**[3], **Rama Rao Amara**[1], **Stella M. Papa**[2,4]

[1]Department of Microbiology and Immunology, Emory Vaccine Center, Yerkes National Primate Research Center, Emory University, Atlanta, Georgia

[2]Yerkes National Primate Research Center, Emory University, Atlanta, Georgia

[3]Center for Drug Discovery, University of Nebraska Medical Center, Omaha, Nebraska

[4]Department of Neurology, Emory University School of Medicine, Atlanta, Georgia

Abstract

Dyskinesia induced by long-term L-Dopa (LID) therapy in Parkinson disease is associated with altered striatal function whose molecular bases remain unclear. Here, a transcriptomic approach was applied for comprehensive analysis of distinctively regulated genes in striatal tissue, their specific pathways, and functional- and disease-associated networks in a rodent model of LID. This approach has identified transforming growth factor beta type 1 (TGFβ1) as a highly upregulated gene in dyskinetic animals. TGFβ1 pathway is a top aberrantly regulated pathway in the striatum following LID development based on differentially expressed genes (> 1.5 fold change and $P < 0.05$). The induction of TGFβ1 pathway specific genes, *TGFβ1, INHBA, AMHR2* and *PMEPA1* was also associated with regulation of *NPTX2, PDP1, SCG2, SYNPR, TAC1, TH, TNNT1* genes. Transcriptional network and upstream regulator analyses have identified AKT-centered functional and ERK-centered disease networks revealing the association of *TGFβ1, IL-1β* and *TNFα* with LID development. Therefore, results support that TGFβ1 pathway is a major contributor to the pathogenic mechanisms of LID.

Correspondence Shetty Ravi Dyavar, Department of Microbiology and Immunology, Emory Vaccine Center, Yerkes National Primate Research Center, Emory University, Atlanta, GA 30329. shettyravi.dyavar@unmc.edu; Stella M. Papa, Yerkes National Primate Research Center, Emory University, Atlanta, GA 30329. spapa@emory.edu.

Present address

Shetty Ravi Dyavar, UNMC Center for Drug Discovery, University of Nebraska Medical Center (UNMC), Omaha, NE

AUTHOR CONTRIBUTIONS

Stella M. Papa and Shetty Ravi Dyavar designed research. Lisa F. Potts and Bhagya Laxmi Dyavar Shetty conducted in vivo experiments and extracted striatal tissue. Shetty Ravi Dyavar performed RNA extraction, microarray, transcriptomic, pathway enrichment, transcriptional networking, upstream regulator analyses. Shetty Ravi Dyavar, Lisa F. Potts, Bhagya Laxmi Dyavar Shetty and Benton Lawson performed reverse transcription polymerase chain reaction (RT-PCR) assays. Courtney V. Fletcher and Anthony T. Podany provided the Ingenuity Pathway Analysis software. Stella M. Papa and Goichi Beck analyzed behavioral data and Rama Rao Amara provided gene spring GX software for transcriptomic data analysis. Shetty Ravi Dyavar and Stella M. Papa wrote the manuscript. All authors reviewed the manuscript.

CONFLICT OF INTEREST

The authors declare no potential conflict of interest.

SUPPORTING INFORMATION

Additional supporting information may be found online in the Supporting Information section at the end of this article.

Keywords

IL-1β; inflammation; INHBa; L-Dopa-induced dyskinesia; NMU; Parkinson disease; TAC1; TGFβ1; TNFα

1 | INTRODUCTION

Parkinson disease (PD) is characterized by motor symptoms that primarily originate from the loss of nigrostriatal dopaminergic neurons. Dopamine replacement by L-Dopa improves motor disability, but is frequently complicated by the appearance of involuntary movements, namely L-Dopa-induced dyskinesia (LID). Although the mechanisms underlying LID development are not completely understood, there is evidence for major regulatory changes of several molecules in the striatum. Elevated levels of the transcription factor *ΔFosB*[1,2] and the phosphorylated forms of (a) dopamine cAMP related phosphoprotein (*pDARPP32*),[3] (b) extracellular signal regulated kinase 1/2 (*pERK 1/2*)[4] and (c) histone H3 (*H 3*)[5] are consistently found in rodent and primate models of LID. These molecules participate in signaling mechanisms of dopamine D1 and D2 receptors. *ΔFosB* is widely overexpressed in striatal cells that express either D1 or D2 receptors. *cAMP/PKA/DARPP-32* and *PKA*/mitogen activated protein kinase extracellular signal regulated kinase (*MEK*)/*ERK 1/2* largely mediate D1R signaling.[3,6-8] Phosphorylated ERK1/2 activates mammalian target of rapamycin complex 1 (*mTORC1*),[9] which is a critical regulator of synaptic plasticity and memory,[10] and plasticity mechanisms are altered in rodent models of LID.[11-13] LID is associated with dysregulation of striatal glutamate transmission.[14] In particular, changes in NMDAR subunits *GluN2A* and *2B* play a key role in altered plasticity mechanisms in both D1R- and D2R-expressing cells.[15-18] Thus, at the cellular level, LID is related to dysfunction in both direct and indirect striatal projection neurons (dSPN and iSPN), which express dopamine D1R and D2R, respectively.[19,20] Signaling from striatal interneurons are dysregulated as a result of glutamatergic and dopaminergic changes, and interneurons majorly drive striatal microcircuits.[13]

In addition, glial mechanisms and inflammatory changes that participate in altered synaptic function[21] are present following chronic L-Dopa treatment,[22-24] suggesting a potential role in LID development. Nevertheless, the mechanisms and mediators of neuroinflammation associated to LID have not been profiled. Global gene expression analyses in animal models[25-29] have been limited to differentially expressed genes and enrichment of regulated pathways without detailing early molecular events. Here, we applied transcriptomic and a combination of pathway enrichment, gene networking and upstream regulator analyses to identify key molecular mediators of LID development. We used chronic L-Dopa treatment in a rodent model of PD to induce abnormal involuntary movements (AIMs), which are equivalent to the primate LID. Pathway enrichment, functional and disease network building and upstream regulator analyses have identified transforming growth factor beta type 1 (*TGFβ1*), interleukin 1 beta (*IL1β*) and tumor necrosis factor alpha (*TNFα*) cytokines as key mediators of chronic inflammation leading to AIMs development in rats.

2 | RESULTS

2.1 | Identification of gene regulation in the striatum of dyskinetic rats

AIMs were evident in the L-Dopa-treated group but not in control saline-treated rats (Figure 1A-C). Baseline contralateral rotation induced by apomorphine was similar between the two groups of rats, and contralateral rotation in the L-Dopa-treated group was robust on day 1 and progressed with daily treatment to a significant difference by day 8 (Figure 1D). Increased expression of striatal ΔFosB, an established LID marker, was confirmed in the L-Dopa-treated group using quantitative polymerase chain reaction (qPCR) (Figure 1E). Consistent with previous reports,[1,2] eight out of nine RNA samples showed a minimum increase of 1.6-fold in *ΔFosB* gene expression normalized to values of control rats. In contrast, no significant changes in *FosB* gene expression were observed between the two groups (Figure 1E). Therefore, the group of chronic L-Dopa treatment expressed correlated behavioral and molecular patterns of the rodent model of LID.

Transcriptomic analysis was performed on RNA extracted from striatal tissue samples derived from L-Dopa-treated and control rats (n = 6 in each group) to identify a list of AIMs-associated genes. Results showed a differential gene expression pattern (Figure 2A). Due to the number of samples (n = 6 per group) and rigorous filtration (1.5 FC and < 0.05 *P* significance), 147 (0.67%) out of 13,374 genes were aberrantly regulated in animals with AIMs (Figure 2A). Among these genes, 110 (0.5%) were upregulated (Table S2), and 37 (0.16%) were downregulated (Table S3). Mapping of differentially expressed transcript IDs to NCBI Entrez gene database in IPA resulted in 108 upregulated and 35 downregulated transcripts of known genes in the database. To understand the differences between transcriptomes of L-Dopa-treated and control groups, we performed principal component analysis on whole transcriptome datasets of mRNA profiles and identified a marked difference between datasets (Figure 2B). Subsequently, we performed functional classification of expressed transcripts to categorize the differentially expressed genes. This analysis showed host genes of enzymes (kinases, phosphatases and peptidases), growth factors, ion channels, chemokines, G-protein coupled receptors, nuclear receptors and transcription factors as major classes of genes associated with AIMs (Figure 2C).

2.2 | Validation of highly regulated *TGFβ1, INHBA, NMU, TIMP1* and *TAC1* genes

We selected *TGFβ1, INHBa, NMU, TIMP-1* and *TAC1* among the upregulated genes in microarray analysis for validation as gene expression changes underlying L-Dopa-induced AIMs. We selected *TGFβ1* because it belongs to a top regulatory TGFβ1 pathway in L-Dopa-treated rats compared with controls, and the *INHBa* gene because of its association with TGFβ1 pathway. We also selected the upregulated *TIMP-1* and *TAC1* genes because of their previously reported role in LID[30,31] and NMU because of its association with neuronal inflammation.[32] The mRNA expression of selected transcripts was validated in quantitative polymerase chain reaction (qPCR) assays. Comparison of threshold cycle (CT) values of these genes normalized with *GAPDH* showed a significant increase in mRNA expression (*INHBA* > 5.5-fold, *TGFβ1* > 4.7, *TAC1* > 4.14, *NMU* > 1.76, *TIMP1* > 1.92) in eight out of nine L-Dopa-treated rats compared with control rats (Figure 3A). These results validated

our microarray-identified upregulated gene profile in association with the development of AIMs in L-Dopa treated rats.

2.3 | Pathway enrichment analysis identifies hyper regulation of *TGFβ1* signaling

We performed pathway enrichment analysis on significantly up and downregulated (1.5-fold, $P < .05$) gene datasets of L-Dopa-treated rats compared with control rats by IPA. *TGFβ1* pathway was identified as a novel top regulatory pathway with modulation of key pathway associated genes (*TGFβ1, INHBA, AMHR2* and *PMEPA1*) in the striatum of L-Dopa treated rats (Table 1; Figure 3B,C). In our dataset, *TH, DUSP26, TGFβ1, CREM, TNNI3, PTGS2* and *PTEN* genes were associated with protein kinase A signaling pathway; ILK signaling (*FN1, RHOQ, PTGS2* and *PTEN*); inhibition of matrix metalloproteinases or MMPs (*TIMP1, MMP14*); protein ubiquitination pathway (*CRYAB, HSPA5, DNAJB5, HSPB1*); melatonin degradation (*POR* and *SULT1A1*); and prostanoid biosynthesis (*PTGS2*) pathways (Table 1 and Figure 3B). These data are consistent with the role of *PKA* signaling in the aberrant neuronal activity underlying LID development in animal models.[3] More importantly, our analysis identified the key role of *TGFβ1* pathway (Figure 3C), which is highly regulated among altered pathways in the striatum of the rodent model of LID.

2.4 | Regulation of gene expression by *AKT*- and ERK-associated transcriptional programs

To investigate operating transcriptional programs in relation to LID, we performed network analysis of upregulated genes (1.5 FC and P value < 0.05) from our microarray results to identify transcription factors (TFs) that control distinct sets of differentially expressed genes in IPA. We identified 36 distinctly regulated genes in a "neuronal" gene network containing the genes regulated during known nervous system disorders with *AKT* as a central regulator (Figure 4A). In this network, *CFLAR, PDYN* and *TAC1* genes were identified as key genes associated with AIMs. We have also identified the ERK centered "neurological" gene network involving 35 upregulated genes associated with "function" of nervous system (Figure 4B). Notably, among the key LID-associated genes identified in this study, *CFLAR, CRYAB, GADD45A, GJB6, TAC1, TH, HSPA5, HTR1B, NPTX2* are known to play a role in neuronal inflammation[31,33-42] and *TAC1* and *TH* are directly associated with PD[31] (Table S4). Therefore, gene networking analyses identified *AKT* and *ERK* centered gene networks in the striatum of L-Dopa-treated rats regulating key transcriptional programs.

2.5 | Role of *TGFβ1, IL-1β* and *TNFα* cytokines in parkinsonian rats with AIMs

In the list of upregulated LID genes, we performed upstream regulator analysis (URA) and found altered expression of distinct cytokines, growth factors and TFs. Chronic inflammatory marker, *TGFβ1* was the top upstream regulatory growth factor that stimulated expression of 25 target genes (4.09 Z score, $P = 4.84 \times 10^{-8}$) from the list of LID genes (Figure 4C and Table S5). Several growth factors, *AGT, BMP2, EGF, FGF2, HGF, IGF1, MSTN, NGF* and *VEGFA* were identified as upstream regulators with a minimum of $P <$ 0.01 and ≥ 2.0 Z score (Table S5). URA has identified significant induction of *IL-1β* (2.41 Z score, $P = 2.77 \times 10^{-11}$) and *TNFα* (2.97 Z score, $P = 2.77 \times 10^{-11}$) inflammatory cytokines that are predicted to stimulate expression of 22 upregulated genes in this rat model of LID (Figure 4D and Table S5). OSM, *IL-1α, IL-5, IL-17α* and *TNFSF11* cytokines were

identified as LID-associated upstream regulators in our analysis (Figure 4D). We found a link between TFs that control expression of multiple genes from the list of differentially expressed genes in our dataset using URA. *CREB1* was identified as a major TF that controls the expression of *NPTX2, SCG2* and *HSPA5* target genes (Figure 4E and Table S5). *GADD45A, HSPA5* and *HTR1B* genes were predicted to be regulated by *TGFβ1*. Interestingly, pro-inflammatory *IL-1β* cytokine that is known to play a key role in multiple neurodegenerative disorders was predicted to control expression of *CFLAR, CRYAB, GADD45a* and *TAC1* LID genes (Table S5). In addition, *TNFα*-controlling *CFLAR, CRYAB, GADD45a, TAC1* and *TH* gene expression showed a direct link between inflammatory cytokines and regulated genes in this rat model of LID (Figure 4E and Table S5). *CREB1* controlling the expression of 23 genes was among the top upstream regulatory TF with high significance (*P* value, 2.6×10^{-16}) and 4.25 Z score (Figure 4E and Table S5). *CEBPα, EGR1, SMAD3, SMARCA4, SP1, STAT3* and *TP53* were among other upregulated TFs with a minimum of 2.0 Z score and 0.01 *P* value significance. *SMAD7* was the only down modulated TF based on upregulated target gene analysis (Table S5). These results showed that inflammatory factors, *TGFβ1, IL-1β* and *TNFα* play a major role in the control of gene expression associated with LID in the rat model of PD.

3 | DISCUSSION

Our integrated transcriptomic analyses revealed a significant contribution of TGFβ1 pathway and other cytokines to the development of AIMs in the rodent model. Although previous studies have provided insights into the gene regulation in relation to the development of LID in animal models,[25,29] the integration of various systems biology tools applied here, including transcriptomic, pathway enrichment, gene networking and URA led to identify important early molecular events in LID development. Konradi et al,[25] utilized L-Dopa (6 mg/kg, i.p.) to induce AIMs in rats with 6-hydroxydopamine hydrobromide (6-OHDA)-lesions, and analyzed striatal gene expression in a smaller set of 8000 transcripts. This study has identified 250 differentially expressed transcripts, but all those genes were moderately regulated (< 1.6 FC) in rats with AIMs. By contrast, Charbonnier-Beupel et al[27] utilized a higher dose of L-Dopa (20 mg/kg, i.p.) in dopamine-depleted mice to analyze the transcriptomic profile of the striatum, which was more consistent with our data showing *NPTX2, TH, NOCT* and *ΔFosB* upregulated genes. Heiman et al. utilized a different approach to identify gene regulation in subpopulations of striatal projection neurons (SPNs), that is, dSPNs expressing dopamine D1 receptors and iSPNs expressing dopamine D2 receptors following low and high doses of L-Dopa treatment in rodents.[43] Interestingly, in this study, several of the genes associated with cyclic AMP-responsive element binding, activator protein 1, *ERK* and inflammatory signaling pathways were highly regulated in dSPNs, but minimal or no changes were observed in iSPNs in L-Dopa-treated rodents with AIMs. These differences may contribute to the specific mechanisms underlying the development of AIMs, since both dSPNs and iSPNs play a role in movement generation,[44,45] but may undergo distinctive dysregulation after chronic L-Dopa treatment.[43] However, the comprehensive approach taken in the present study allowed us to uncover operating transcriptional programs and upstream regulated genes in the striatum associated with the dyskinesias of parkinsonian rats.

Patients with Parkinson disease are treated with variable L-Dopa doses that range from 400 to 800 mg per day on average,[46] and LID develops gradually during chronic therapy.[47] However, the onset and the severity of LID are not strictly dependent on the L-Dopa dose, but rather related to a combination of factors, including disease progression and the presence of hypersensitive motor responses.[48] Based on FDA dose equivalence, the human equivalent rat dose could be estimated between 40 and 80 mg/kg, but the L-Dopa doses commonly used in rat models of PD to reproduce LID are much lower (8–25 mg/kg).[25,27,43] Unilateral 6-OHDA lesion of the median forebrain bundle (MFB) creates a unique model of complete dopamine denervation on one side of the brain (> 95% nigral cell loss), which results in very high sensitivity to dopaminergic stimulation and lower dose requirements.[49,50] In this model, LID can be observed even with the first L-Dopa dose in some animals and fully develops within days of daily administration in the majority of animals.[2,51] We selected to use L-Dopa at 25 mg/kg twice daily to induce consistent expression of all categories of AIMs across animals since lower doses can induce variable severity of AIMs in only 50% of animals.[52] A robust motor response with dyskinesias was critical to conduct a mechanistic study using microarray technologies. The present data show that the development of robust AIMs by chronic L-Dopa treatment (25 mg/kg, i.p.) in rats was associated with gene regulation of pro-inflammatory mediators.

Elevated levels of *TGFβ1, IL-1-β* and *TNFα,* all markers of inflammation, were reported in cerebrospinal fluid and brain tissue of patients with PD and exposed to chronic L-Dopa treatment.[53-55] *TGFβ1* is a pleiotropic cytokine that induces pro- and anti-inflammatory responses depending on the pathological context. *TGFβ1* activation can be neuroprotective against MPTP toxicity in mice,[56] an effect likely mediated by its upregulation following the adaptive transfer of regulatory T cells (CD4 + CD25hi), which control the function of T cells, increasing the levels of glial cell derived neurotrophic factor (*GDNF*).[57] Additionally, *TGFβ1* deficiency leads to age-related degeneration of the nigrostriatal system.[56] Therefore, *TGFβ1* possesses anti-inflammatory effects in the context of PD. The upregulation of the *TGFβ1* gene along with pathway specific genes (*INHBA, AMHR2* and *PMEPA1*) in the present study indicates the role of *TGFβ1* pathway in inflammatory response occurring in chronic L-Dopa treatment and the development of AIMs in rats. Microglia and macrophages are the major source of *TGFβ1* production in the brain.[57] Congruent with these data, a recent study reported marked astrocytosis associated with inflammation in the striatum of dyskinetic rats.[23] Multiple inflammatory factors may participate in the inflammation of brain tissue, but the role of L-Dopa and advanced (or progression of) neurodegenerative changes in the activation of cytokine mediators needs further investigation.

Increased glutamatergic neurotransmission is thought to play a role in the development of dyskinesia, and amantadine, which has NMDA antagonistic actions, has antidyskinetic effects.[58] The beneficial effects of Amantadine is partially attributed to inhibition of inflammation caused by microglia in the brain of animal models of PD.[59] Therefore, inflammation could play a major role in the adaptive glutamatergic changes developed during chronic L-Dopa treatment and likely associated with LID. Our analysis showed that the *5-HT1B* gene (*HTR1B*) was induced by chronic L-Dopa treatment. Eltoprazine, a selective partial agonist at 5-HT1A and 5-HT1B receptors has showed a significant reduction of LID in animal models,[60] and importantly in a dose-response study conducted in

patients with PD.[61] Our data are consistent with Zhang et al[62] findings of upregulated *HTR1B* mRNA expression in rodents after dopamine loss and L-Dopa treatment. Interestingly, *HTR1B* may promote migration of pro-inflammatory monocytes and dendritic cells into lymphoid tissues[63] and also causing airway inflammation.[64] However, further studies are necessary to evaluate the role of *HTR1B* in the chronic inflammation associated with LID. Gene network analyses provided additional evidence that key genes involved in neuronal inflammation, including *CFLAR, CRYAB, GADD45A, GJB6, HSPA5, HTR1B, NPTX2, TAC1* and *TH* were induced in the striatum of dyskinetic rats. Notably, both non-physiologic levels of dopamine due to L-Dopa treatment and significant glutamate dysregulation in advanced PD are known to create a cytokine mediated pro-inflammatory microenvironment in the striatum.[65] Particularly, treatment in the form of non-physiologic pulsatile dopaminergic stimulation by L-Dopa that induces clear LID is also associated with neuroinflammation.[22] Elevated levels of cytokines *IL-1β, TNFα* and *TGFβ1* may coexist at different stages of PD.[66] Migration of immune cells into the brain or immune cell activation during chronic L-Dopa treatment may contribute to the upregulated inflammatory mediators.[66] A role of TNFα and IL-1β cytokines in PD pathology has been reported in recent studies.[67-69] Data of early exposure to anti-TNFα therapy in patients with inflammatory bowel disease showed substantially reduced PD incidence.[67] Furthermore, administration of TNFα specific inhibitor, XPro1595 to hemiparkinsonian rats reduced nigral cell loss and glial activation, indicating a mechanistic improvement of PD pathology.[68] Activation of IL-1 pathway has been associated with dopamine loss and parkinsonism during aging, and reduction of IL-1 activity may have neuroprotective effects.[69] Conceivably, these inflammatory mediators could play a role in modulating adaptive changes during chronic L-Dopa treatment. The transcriptomic analyses performed here revealed a prominent regulation of the *TGFβ1* pathway during chronic L-Dopa treatment. While there is no evidence for effects of anti-TNFα, anti-IL-1β and anti-TGFβ1 therapies on LID, the available data warrant investigations of these agents for specific antidyskinetic actions. The present data also support further studies to dissect the inflammatory mechanisms associated with LID.

4 | MATERIALS AND METHODS

4.1 | Experimental model and subject details

Male Sprague-Dawley rats (150-250 g weight) were purchased from Charles River, Wilmington, Massachusetts and were housed at the Yerkes National Primate Research Center (YNPRC), Emory University with free access to food and water, 12 hours light/dark cycles, constant temperature and humidity. Animal maintenance and procedures were in accordance with the National Institutes of Health (NIH) Guide for the Care and Use of Laboratory Animals and approved by the institutional animal care and use committee (IACUC). Deeply anesthetized rats were surgically injected with 6-hydroxydopamine (6-OHDA) (Sigma–Aldrich, St. Louis, Missouri) unilaterally into the medial forebrain bundle under stereotactic guidance, as described previously.[70] Three weeks after the surgery, the rotational response to a subthreshold dose of apomorphine (0.05 mg/kg, s.c.) (Sigma–Aldrich, St. Louis, Missouri) was determined to assess the extent of the lesion. Rats with more than 100 contralateral 360° turns compatible with a full lesion (>95% dopamine cell

loss) were selected for the study and divided into two groups, chronic L-Dopa or saline (control) treatment. L-Dopa methyl ester plus benserazide (25 mg/kg and 6.25 mg/kg), respectively, Sigma–Aldrich, St. Louis, Missouri) or saline was administered through intraperitoneal (i.p.) route twice daily for eight days to develop maximal motor behavioral responses in rats.

4.2 | Behavioral assessment

Both groups of rats (L-Dopa treated, n = 9, and saline-treated controls, n = 9) were assessed for their movement disorder related responses to L-Dopa on days 1 and 8 of daily L-Dopa treatment. Control rats received L-Dopa only on test days 1 and 8, the other days they received only saline twice daily. AIMs were scored using a standardized scale including the classic categories: (a) limb dyskinesias; (b) axial dystonia; and (c) masticatory (orolingual) dyskinesias that were graded from score 0 to 4. Each category was scored 0 to 4 (0 is absent; 1 is occasionally present and lasting ≤ 30 sec; 2 is occasionally present and lasting ≥ 30 sec; 3 is frequently present and lasting ≥ 30 sec or continuous but may be interrupted by strong sensory distractions; and 4 is continuous and not interrupted by strong sensory distraction.[29,71] Animals were observed and scored directly by an examiner every 15 minute for 210 minutes after L-Dopa injection on test days 1 and 8. Scores in each interval were added to obtain a total value of the AIMs category for each animal in each test. Contralateral rotation was assessed as described before[2] at day 1 and 8, and only turns of completed 360° were counted. Contraversive rotation was not included in the analysis of total AIMs because it also represents the antiparkinsonian effect of L-Dopa.[48] Rotational behavior was measured using an automated rotometer for the whole duration of the L-Dopa response. Full circle rotations contralateral to the lesion were computed for analysis of L-Dopa responses. Total rotation was the sum of complete contraversive turns measured every 5 minute interval for the entire L-Dopa response.

4.3 | RNA extraction and microarray procedures

All eighteen rats were sacrificed on day 8 post L-Dopa (treated group) or saline (controls) treatment. Brains were rapidly removed, and the striatum was dissected on ice, immediately stored at −80°C until processed for RNA extraction. Total RNA was extracted from striatal tissue ipsilateral to the 6-OHDA lesion of chronic L-Dopa-treated rats and saline-treated rats (controls) using Qiagen RNeasy fibrous tissue mini kit (Qiagen, USA). On-column RNase free DNAse digestion for DNA clean-up from RNA was also included according to the manufacturer's protocol. RNA integrity was analyzed with Bioanalyzer (Agilent Technologies, USA), and all samples showed >9.0 RNA integrity number, which indicated their high quality for downstream applications. Concentration of extracted RNA was assessed with Nanodrop spectrophotometer (Nanodrop Technologies, USA) according to the manufacturer's protocol. A total of 17 striatal tissue samples (n = 9 from L-Dopa treated group and n = 8 from untreated controls) yielded high RNA concentration and were used in subsequent microarray or qPCR assays. Six RNA samples from each rat group were randomly selected for microarrays that were performed at the Emory integrated genomics core facility at the Emory University as previously described.[72,73] A total of 1 μg of RNA of each sample was reverse transcribed into double stranded complimentary DNA (cDNA) using the cDNA library construction kit (Affymetrix, USA). The cDNA was fragmented and

labeled with biotin using Genechip WT terminal labeling kit (Affymetrix, USA). Biotin-labeled single stranded cDNA samples were hybridized to an Illumina genechip RatRef-12 v1 expression bead chip, a whole genome gene expression array containing more than 22 000 probes per array targeting genes and alternative splice variants. Array hybridization and wash was performed using genechip R hybridization, wash and stain Kit (Affymetrix, USA) in Hybridization Oven 645 (Affymetrix, USA), and Fluidics Station 450 (Affymetrix, USA) according to the manufacturer's instructions. Slides were scanned by genechip R scanner 3000 (Affymetrix, USA), which generated raw data CEL and CHP files.

4.4 | Microarray analysis

Raw data CEL and CHP files originated from microarray experiments on striatal tissue mRNA derived from L-Dopa (treated group) or saline (controls)-treated rats were analyzed in the Genespring GX10 (GGX10) software (Agilent technologies, USA) and preprocessed them with Robust Multiarray Analysis as previously described.[72,73] In this analysis, the back ground signal correction, per gene normalization to median and probe set summarization was performed. The GGX10 software was also used to analyze genes differentially expressed between L-Dopa (treated group) or saline (controls)-treated groups of rats. The differentially expressed genes were determined by comparing the gene expression intensity profiles of each gene in the L-Dopa-treated group of rats with saline-treated controls. Statistical significance analysis was performed using t test with the filters of $P \leq 0.05$, and 1.5 FC. Principal component analysis (PCA) was performed to identify the difference between overall transcriptomic changes between the L-Dopa treated versus control group of rats in the GGX10 software according to the manufacturer's protocol.

4.5 | Pathway enrichment, network and upstream regulator analyses

We used the Ingenuity Pathway Analysis (IPA) software (Agilent technologies, USA) to enrich pathways, identify gene networks and upstream transcriptional regulators in our differentially expressed genes. First, “core analysis” was performed on the list of differentially expressed up and down regulated genes (0.05*P*, 1.5 FC) in separate analyses to interpret biological pathways as previously described[72] and identify gene networks. Pathways that are regulated due to induction or inhibition of genes associated with them and showed a minimum of <0.05 *P* value significance in their change were considered as influenced pathways during L-DOPA treatment as compared to the saline-treated controls. We generated gene networks by core analysis of LID responsive genes during our “comparative analysis” with controls to find a link among each of the neurological function and disease associated networks. Upstream regulator analysis (URA) of genes was performed in IPA to identify significantly (0.01 P) regulated upstream regulators, such as cytokines, growth factors and transcription factors (TFs), to differentially expressed LID genes with significant Z score (>2.0) that could predict their activation status using IPA software.

4.6 | Quantitative real-time PCR

Total RNA extracted from striatal tissue of L-Dopa-treated rats or control saline-treated rats was reverse transcribed to synthesize cDNA using VILO cDNA synthesis kit (Invitrogen, USA) according to the manufacturer's protocol. Real-time PCR on cDNA samples was

performed in 384 well plate format using a standard protocol in applied biosystems 7900HT instrument. We performed SYBR Green PCRs for *FOSB, ΔFOSB, INHBA, NMU, TAC1, TGFβ1* and *TIMP1* genes using primers listed in Table S1. PCR cycles include, a single initial hot start cycle at 95°C for 5 minute followed by 40 repeats of denaturation (95°C, 15 seconds), primer annealing (55°C, 15 seconds) and DNA synthesis cycles (72°C, 30 seconds). After 40 cycles, an extension step was performed at 72°C for 10 minute and a final step of DNA polymerase deactivation step at 95°C for 5 min. FC in mRNA expression level of each sample was determined using ΔΔCT method[74] and *GAPDH* was used as internal control in qPCR assays. Three minimum replicates were used for all samples in qPCR assays (n = 3).

4.7 | Quantification and statistical analysis

Behavioral data were analyzed with two-way ANOVA for repeated measures followed by post-hoc PLSD tests if the ANOVA 'f' indicated significance. In transcriptomic analyses, six chronic LID rats (n = 6) were compared with PD controls. Genes that were differentially expressed in the striatal tissue of rats with AIMs as compared to their PD counterparts (saline treated rats without AIMs) with a minimum of 1.5 FC and 0.05 *P* value using unpaired *t* test were considered significant. Then, significantly regulated genes were used to identify differentially regulated pathways and upstream regulators using IPA. t tests were used to compare differences in microarray profiles between two animal groups. IPA generates a wide array of pathways, and to increase the specificity of identified regulated pathways, we used 0.05 *P* value significance filter.

Supplementary Material

Refer to Web version on PubMed Central for supplementary material.

ACKNOWLEDGMENTS

This work was supported by NIH grants NS073994, NS045962 and OD011132 to S. M. P., and P30 MH062261 and Nebraska Research Initiative (NRI) Collaborative Award to S. R. D.

DATA AVAILABILITY STATEMENT

The microarray data that support the findings of this study are openly available in NCBI GSE139438.

REFERENCES

1. Andersson M, Westin JE, Cenci MA. Time course of striatal DeltaFosB-like immunoreactivity and prodynorphin mRNA levels after discontinuation of chronic dopaminomimetic treatment. Eur J Neurosci. 2003;17(3):661–666. [PubMed: 12581184]
2. Cao X, Yasuda T, Uthayathas S, et al. Striatal overexpression of DeltaFosB reproduces chronic levodopa-induced involuntary movements. J Neurosci. 2010;30(21):7335–7343. [PubMed: 20505100]
3. Santini E, Valjent E, Usiello A, et al. Critical involvement of cAMP/DARPP-32 and extracellular signal-regulated protein kinase signaling in L-DOPA-induced dyskinesia. J Neurosci. 2007;27(26):6995–7005. [PubMed: 17596448]

4. Gerfen CR, Miyachi S, Paletzki R, Brown P. D1 dopamine receptor supersensitivity in the dopamine-depleted striatum results from a switch in the regulation of ERK1/2/MAP kinase. J Neurosci. 2002; 22(12):5042–5054. [PubMed: 12077200]
5. Santini E, Heiman M, Greengard P, Valjent E, Fisone G. Inhibition of mTOR signaling in Parkinson's disease prevents L-DOPA-induced dyskinesia. Sci Signal. 2009;2(80):ra36. [PubMed: 19622833]
6. Pavon N, Martin AB, Mendialdua A, Moratalla R. ERK phosphorylation and FosB expression are associated with L-DOPA-induced dyskinesia in hemiparkinsonian mice. Biol Psychiatry. 2006;59(1):64–74. [PubMed: 16139809]
7. Westin JE, Vercammen L, Strome EM, Konradi C, Cenci MA. Spatio-temporal pattern of striatal ERK1/2 phosphorylation in a rat model of L-DOPA-induced dyskinesia and the role of dopamine D1 receptors. Biol Psychiatry. 2007;62(7):800–810. [PubMed: 17662258]
8. Chen X, McCorvy JD, Fischer MG, et al. Discovery of G protein-biased D2 dopamine receptor partial agonists. J Med Chem. 2016; 59(23):10601–10618. [PubMed: 27805392]
9. Carriere A, Cargnello M, Julien LA, et al. Oncogenic MAPK signaling stimulates mTORC1 activity by promoting RSK-mediated raptor phosphorylation. Curr Biol. 2008;18(17):1269–1277. [PubMed: 18722121]
10. Kelleher RJ 3rd, Govindarajan A, Jung HY, Kang H, Tonegawa S. Translational control by MAPK signaling in long-term synaptic plasticity and memory. Cell. 2004;116(3):467–479. [PubMed: 15016380]
11. Calabresi P, Pisani A, Mercuri NB, Bernardi G. The corticostriatal projection: from synaptic plasticity to dysfunctions of the basal ganglia. Trends Neurosci. 1996;19(1):19–24. [PubMed: 8787136]
12. Picconi B, Centonze D, Hakansson K, et al. Loss of bidirectional striatal synaptic plasticity in L-DOPA-induced dyskinesia. Nat Neurosci. 2003;6(5):501–506. [PubMed: 12665799]
13. Fieblinger T, Graves SM, Sebel LE, et al. Cell type-specific plasticity of striatal projection neurons in parkinsonism and L-DOPA-induced dyskinesia. Nat Commun. 2014;5:5316. [PubMed: 25360704]
14. Singh A, Jenkins MA, Burke KJ Jr, et al. Glutamatergic tuning of hyperactive striatal projection neurons controls the motor response to dopamine replacement in parkinsonian primates. Cell Rep. 2018; 22(4):941–952. [PubMed: 29386136]
15. Boldry RC, Papa SM, Kask AM, Chase TN. MK-801 reverses effects of chronic levodopa on D1 and D2 dopamine agonist-induced rotational behavior. Brain Res. 1995;692(1-2):259–264. [PubMed: 8548312]
16. Papa SM. The cannabinoid system in Parkinson's disease: multiple targets to motor effects. Exp Neurol. 2008;211(2):334–338. [PubMed: 18433745]
17. Calabresi P, Di Filippo M, Ghiglieri V, Tambasco N, Picconi B. Levodopa-induced dyskinesias in patients with Parkinson's disease: filling the bench-to-bedside gap. Lancet Neurol. 2010;9(11):1106–1117. [PubMed: 20880751]
18. Han C, Nie S, Chen G, et al. Intrastriatal injection of ionomycin profoundly changes motor response to l-DOPA and its underlying molecular mechanisms. Neuroscience. 2017;340:23–33. [PubMed: 27771532]
19. Singh A, Liang L, Kaneoke Y, Cao X, Papa SM. Dopamine regulates distinctively the activity patterns of striatal output neurons in advanced parkinsonian primates. J Neurophysiol. 2015;113(5):1533–1544. [PubMed: 25505120]
20. Cortes M, Malave L, Castello J, et al. CK2 oppositely modulates l-DOPA-induced dyskinesia via striatal projection neurons expressing D1 or D2 receptors. J Neurosci. 2017;37(49):11930–11946. [PubMed: 29097596]
21. Beattie EC, Stellwagen D, Morishita W, et al. Control of synaptic strength by glial TNFalpha. Science. 2002;295(5563):2282–2285. [PubMed: 11910117]
22. Mulas G, Espa E, Fenu S, et al. Differential induction of dyskinesia and neuroinflammation by pulsatile versus continuous l-DOPA delivery in the 6-OHDA model of Parkinson's disease. Exp Neurol. 2016;286:83–92. [PubMed: 27697481]

23. Carta AR, Mulas G, Bortolanza M, et al. L-DOPA-induced dyskinesia and neuroinflammation: do microglia and astrocytes play a role? Eur J Neurosci. 2017;45(1):73–91. [PubMed: 27859864]
24. Pisanu A, Boi L, Mulas G, Spiga S, Fenu S, Carta AR. Neuroinflammation in L-DOPA-induced dyskinesia: beyond the immune function. J Neural Transm (Vienna). 2018;125(8):1287–1297. [PubMed: 29541852]
25. Konradi C, Westin JE, Carta M, et al. Transcriptome analysis in a rat model of L-DOPA-induced dyskinesia. Neurobiol Dis. 2004;17(2):219–236. [PubMed: 15474360]
26. Wang Y, Zhang QJ, Wang HS, Wang T, Liu J. Genome-wide microarray analysis identifies a potential role for striatal retrograde endo-cannabinoid signaling in the pathogenesis of experimental L-DOPA-induced dyskinesia. Synapse. 2014;68(8):332–343. [PubMed: 24599755]
27. Charbonnier-Beaupel F, Malerbi M, Alcacer C, et al. Gene expression analyses identify Narp contribution in the development of L-DOPA-induced dyskinesia. J Neurosci. 2015;35(1):96–111. [PubMed: 25568106]
28. Smith LM, Parr-Brownlie LC, Duncan EJ, et al. Striatal mRNA expression patterns underlying peak dose L-DOPA-induced dyskinesia in the 6-OHDA hemiparkinsonian rat. Neuroscience. 2016;324:238–251. [PubMed: 26968766]
29. Chen G, Nie S, Han C, et al. Antidyskinetic effects of MEK inhibitor are associated with multiple neurochemical alterations in the striatum of Hemiparkinsonian rats. Front Neurosci. 2017;11:112. [PubMed: 28337120]
30. Lorenzl S, Albers DS, Narr S, Chirichigno J, Beal MF. Expression of MMP-2, MMP-9, and MMP-1 and their endogenous counterregulators TIMP-1 and TIMP-2 in postmortem brain tissue of Parkinson's disease. Exp Neurol. 2002;178(1):13–20. [PubMed: 12460604]
31. Wang Q, Chu CH, Qian L, et al. Substance P exacerbates dopaminergic neurodegeneration through neurokinin-1 receptor-independent activation of microglial NADPH oxidase. J Neurosci. 2014;34(37):12490–12503. [PubMed: 25209287]
32. Cardoso V, Chesne J, Ribeiro H, et al. Neuronal regulation of type 2 innate lymphoid cells via neuromedin U. Nature. 2017;549(7671):277–281. [PubMed: 28869974]
33. Rodriguez-Grande B, Blackabey V, Gittens B, Pinteaux E, Denes A. Loss of substance P and inflammation precede delayed neurodegeneration in the substantia nigra after cerebral ischemia. Brain Behav Immun. 2013;29:51–61. [PubMed: 23232501]
34. Xiaohong W, Jun Z, Hongmei G, Fan Q. CFLAR is a critical regulator of cerebral ischaemia-reperfusion injury through regulating inflammation and endoplasmic reticulum (ER) stress. Biomed Pharmacother. 2019;117:109155. [PubMed: 31387178]
35. Shao W, Zhang SZ, Tang M, et al. Suppression of neuroinflammation by astrocytic dopamine D2 receptors via alphaB-crystallin. Nature. 2013;494(7435):90–94. [PubMed: 23242137]
36. Di Giovanni S, Knoblach SM, Brandoli C, Aden SA, Hoffman EP, Faden AI. Gene profiling in spinal cord injury shows role of cell cycle in neuronal death. Ann Neurol. 2003;53(4):454–468. [PubMed: 12666113]
37. Fujita A, Yamaguchi H, Yamasaki R, et al. Connexin 30 deficiency attenuates A2 astrocyte responses and induces severe neurodegeneration in a 1-methyl-4-phenyl-1,2,3,6-tetrahydropyridine hydrochloride Parkinson's disease animal model. J Neuroinflammation. 2018;15(1):227. [PubMed: 30103794]
38. Sun Q, Wang S, Chen J, et al. MicroRNA-190 alleviates neuronal damage and inhibits neuroinflammation via Nlrp3 in MPTP-induced Parkinson's disease mouse model. J Cell Physiol. 2019;234(12):23379–23387. [PubMed: 31232472]
39. Tabrez S, Jabir NR, Shakil S, et al. A synopsis on the role of tyrosine hydroxylase in Parkinson's disease. CNS Neurol Disord Drug Targets. 2012;11(4):395–409. [PubMed: 22483313]
40. Enogieru AB, Omoruyi SI, Hiss DC, Ekpo OE. GRP78/BIP/HSPA5 as a therapeutic target in models of Parkinson's disease: a mini review. Adv Pharmacol Sci. 2019;2019:2706783. [PubMed: 30949202]
41. Sibille E, Su J, Leman S, et al. Lack of serotonin1B receptor expression leads to age-related motor dysfunction, early onset of brain molecular aging and reduced longevity. Mol Psychiatry. 2007;12(11):1042–1056, 1975. [PubMed: 17420766]

42. Moran LB, Hickey L, Michael GJ, et al. Neuronal pentraxin II is highly upregulated in Parkinson's disease and a novel component of Lewy bodies. Acta Neuropathol. 2008;115(4):471–478. [PubMed: 17987278]
43. Heiman M, Heilbut A, Francardo V, et al. Molecular adaptations of striatal spiny projection neurons during levodopa-induced dyskinesia. Proc Natl Acad Sci U S A. 2014;111(12):4578–4583. [PubMed: 24599591]
44. Uthayathas S, Masilamoni GJ, Shaffer CL, Schmidt CJ, Menniti FS, Papa SM. Phosphodiesterase 10A inhibitor MP-10 effects in primates: comparison with risperidone and mechanistic implications. Neuropharmacology. 2014;77:257–267. [PubMed: 24490227]
45. Cui G, Jun SB, Jin X, et al. Concurrent activation of striatal direct and indirect pathways during action initiation. Nature. 2013;494(7436):238–242. [PubMed: 23354054]
46. Brodell DW, Stanford NT, Jacobson CE, Schmidt P, Okun MS. Carbidopa/levodopa dose elevation and safety concerns in Parkinson's patients: a cross-sectional and cohort design. BMJ Open. 2012;2(6):e001971.
47. Rascol O, Brooks DJ, Korczyn AD, De Deyn PP, Clarke CE, Lang AE. A five-year study of the incidence of dyskinesia in patients with early Parkinson's disease who were treated with ropinirole or levodopa. N Engl J Med. 2000;342(20):1484–1491. [PubMed: 10816186]
48. Nutt JG, Brodsky MA. Dyskinesia induced by levodopa and dopamine agonists in patients with Parkinson's disease. In: Factor AA, Lang AE, Weiner WJ, eds. Drug-Induced Movement Disorders. Blackwell; 2005:313–350. https://onlinelibrary.wiley.com/doi/abs/10.1002/9780470753217.ch13
49. Papa SM, Engber TM, Kask AM, Chase TN. Motor fluctuations in levodopa treated parkinsonian rats: relation to lesion extent and treatment duration. Brain Res. 1994;662(1-2):69–74. [PubMed: 7859092]
50. Andersson M, Hilbertson A, Cenci MA. Striatal fosB expression is causally linked with l-DOPA-induced abnormal involuntary movements and the associated upregulation of striatal prodynorphin mRNA in a rat model of Parkinson's disease. Neurobiol Dis. 1999;6(6):461–474. [PubMed: 10600402]
51. Crittenden JR, Cantuti-Castelvetri I, Saka E, et al. Dysregulation of CalDAG-GEFI and CalDAG-GEFII predicts the severity of motor side-effects induced by anti-parkinsonian therapy. Proc Natl Acad Sci U S A. 2009;106(8):2892–2896. [PubMed: 19171906]
52. Cenci MA, Lee CS, Bjorklund A. L-DOPA-induced dyskinesia in the rat is associated with striatal overexpression of prodynorphin- and glutamic acid decarboxylase mRNA. Eur J Neurosci. 1998;10(8):2694–2706. [PubMed: 9767399]
53. Mogi M, Harada M, Narabayashi H, Inagaki H, Minami M, Nagatsu T. Interleukin (IL)-1 beta, IL-2, IL-4, IL-6 and transforming growth factor-alpha levels are elevated in ventricular cerebrospinal fluid in juvenile parkinsonism and Parkinson's disease. Neurosci Lett. 1996;211(1):1. [PubMed: 8809833]
54. Vawter MP, Dillon-Carter O, Tourtellotte WW, Carvey P, Freed WJ. TGFbeta1 and TGFbeta2 concentrations are elevated in Parkinson's disease in ventricular cerebrospinal fluid. Exp Neurol. 1996;142(2):313–322. [PubMed: 8934562]
55. Nagatsu T, Mogi M, Ichinose H, Togari A. Cytokines in Parkinson's disease. J Neural Transm Suppl. 2000;(58):143–151. 10.1007/978-3-7091-6284-2_12 [PubMed: 11128604]
56. Tesseur I, Nguyen A, Chang B, et al. Deficiency in neuronal TGF-beta signaling leads to nigrostriatal degeneration and activation of TGF-beta signaling protects against MPTP neurotoxicity in mice. J Neurosci. 2017;37(17):4584–4592. [PubMed: 28363982]
57. Reynolds AD, Banerjee R, Liu J, Gendelman HE, Mosley RL. Neuroprotective activities of CD4+CD25+ regulatory T cells in an animal model of Parkinson's disease. J Leukoc Biol. 2007;82(5):1083–1094. [PubMed: 17675560]
58. Meissner WG, Frasier M, Gasser T, et al. Priorities in Parkinson's disease research. Nat Rev Drug Discov. 2011;10(5):377–393. [PubMed: 21532567]
59. Kim JH, Lee HW, Hwang J, et al. Microglia-inhibiting activity of Parkinson's disease drug amantadine. Neurobiol Aging. 2012;33(9):2145–2159. [PubMed: 22035588]

60. Bezard E, Tronci E, Pioli EY, et al. Study of the antidyskinetic effect of eltoprazine in animal models of levodopa-induced dyskinesia. Mov Disord. 2013;28(8):1088–1096. [PubMed: 23389842]
61. Svenningsson P, Rosenblad C, af Edholm Arvidsson K, et al. Eltoprazine counteracts L-DOPA-induced dyskinesias in Parkinson's disease: a dose-finding study. Brain. 2015;138(4):963–973. [PubMed: 25669730]
62. Zhang X, Andren PE, Greengard P, Svenningsson P. Evidence for a role of the 5-HT1B receptor and its adaptor protein, p11, in L-DOPA treatment of an animal model of parkinsonism. Proc Natl Acad Sci U S A. 2008;105(6):2163–2168. [PubMed: 18256188]
63. Muller T, Durk T, Blumenthal B, et al. 5-hydroxytryptamine modulates migration, cytokine and chemokine release and T-cell priming capacity of dendritic cells in vitro and in vivo. PLoS One. 2009;4(7):e6453. [PubMed: 19649285]
64. Müller T, Huttel A, Grimm M, Idzko M. The serotoninergic receptor subtype 5-HTR1B contributes to the pathogenesis of allergic airway inflammation. Eur Respir J. 2012;40:P3740.
65. Robelet S, Melon C, Guillet B, Salin P, Kerkerian-Le Goff L. Chronic L-DOPA treatment increases extracellular glutamate levels and GLT1 expression in the basal ganglia in a rat model of Parkinson's disease. Eur J Neurosci. 2004;20(5):1255–1266. [PubMed: 15341597]
66. Imamura K, Hishikawa N, Sawada M, Nagatsu T, Yoshida M, Hashizume Y. Distribution of major histocompatibility complex class II-positive microglia and cytokine profile of Parkinson's disease brains. Acta Neuropathol. 2003;106(6):518–526. [PubMed: 14513261]
67. Peter I, Dubinsky M, Bressman S, et al. Anti-tumor necrosis Factor therapy and incidence of Parkinson disease among patients with inflammatory bowel disease. JAMA Neurol. 2018;75(8):939–946. [PubMed: 29710331]
68. Barnum CJ, Chen X, Chung J, et al. Peripheral administration of the selective inhibitor of soluble tumor necrosis factor (TNF) XPro(R) 1595 attenuates nigral cell loss and glial activation in 6-OHDA hemiparkinsonian rats. J Parkinsons Dis. 2014;4(3):349–360. [PubMed: 25061061]
69. Stojakovic A, Paz-Filho G, Arcos-Burgos M, Licinio J, Wong ML, Mastronardi CA. Role of the IL-1 pathway in dopaminergic neurodegeneration and decreased voluntary movement. Mol Neurobiol. 2017;54(6):4486–4495. [PubMed: 27356916]
70. Papa SM, Boldry RC, Engber TM, Kask AM, Chase TN. Reversal of levodopa-induced motor fluctuations in experimental parkinsonism by NMDA receptor blockade. Brain Res. 1995;701(1–2):13–18. [PubMed: 8925275]
71. Lee CS, Cenci MA, Schulzer M, Bjorklund A. Embryonic ventral mesencephalic grafts improve levodopa-induced dyskinesia in a rat model of Parkinson's disease. Brain. 2000;123(Pt 7):1365–1379. [PubMed: 10869049]
72. Kwa S, Kannanganat S, Nigam P, et al. Plasmacytoid dendritic cells are recruited to the colorectum and contribute to immune activation during pathogenic SIV infection in rhesus macaques. Blood. 2011;118(10):2763–2773. [PubMed: 21693759]
73. Dyavar Shetty R, Velu V, Titanji K, et al. PD-1 blockade during chronic SIV infection reduces hyperimmune activation and microbial translocation in rhesus macaques. J Clin Invest. 2012;122(5):1712–1716. [PubMed: 22523065]
74. Dyavar SR, Ye Z, Byrareddy SN, et al. Normalization of cell associated antiretroviral drug concentrations with a novel RPP30 droplet digital PCR assay. Sci Rep. 2018;8(1):3626. [PubMed: 29483619]

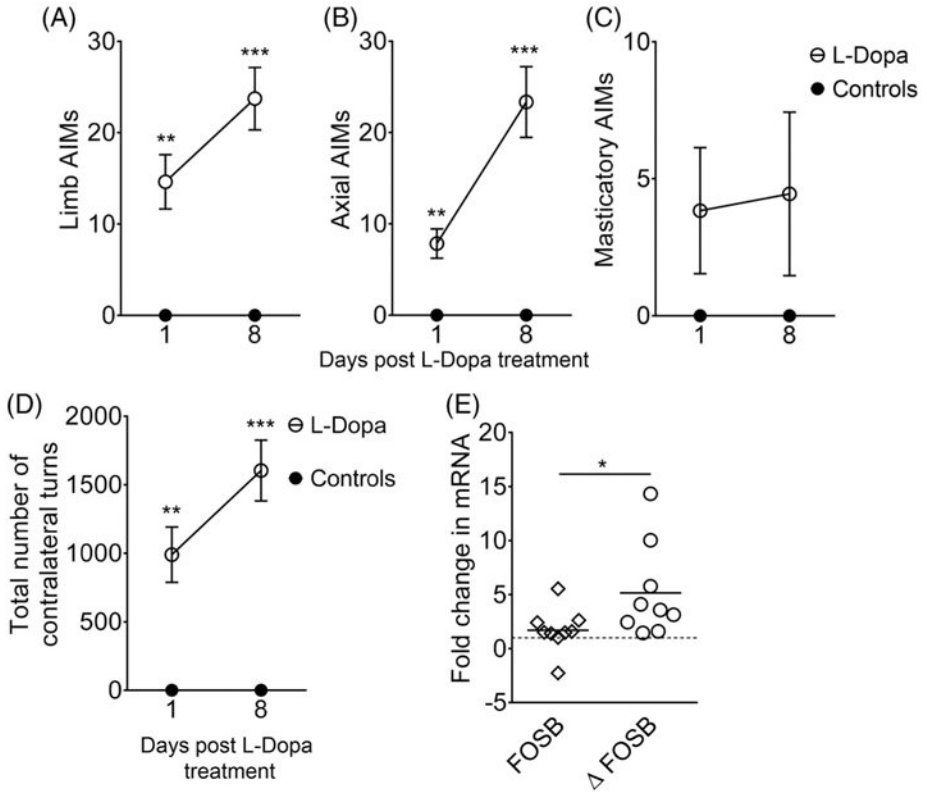

FIGURE 1.

Behavioral assessment of motor responses to L-Dopa. Limb, A; axial, B; masticatory, C, abnormal involuntary movements (AIMs); and the total number of contralateral turns, D, in L-Dopa- and saline-treated groups of rats with unilateral 6-hydroxydopamine hydrobromide (6-OHDA) lesion of the nigrostriatal pathway are shown (Materials and Methods). Chronic L-Dopa administration (25 mg/kg, ip) induced significant AIMs, which progressed from day 1 to day 8 of daily treatment. The control group received daily saline injections (rats in both groups have similar baseline rotational responses to apomorphine before starting daily L-Dopa treatment). ** 0.01 *P* and *** 0.001 *P* vs control group (n = 9 each group). Data are mean ± SEM. E, Quantitative rerverse transcription polymerase chain reaction (RT-PCR) analysis of striatal *FOSB* and *ΔFOSB* transcripts in L-Dopa-treated rats are depicted as fold change in mRNA expression compared with controls (average mRNA expression in saline-treated rats). The mRNA expression of each animal was normalized to *GAPDH* internal control as described in material and methods. * 0.05 *P* between *FOSB* and *ΔFOSB* transcripts in the L-Dopa-treated group. Fold change baseline was set to 1

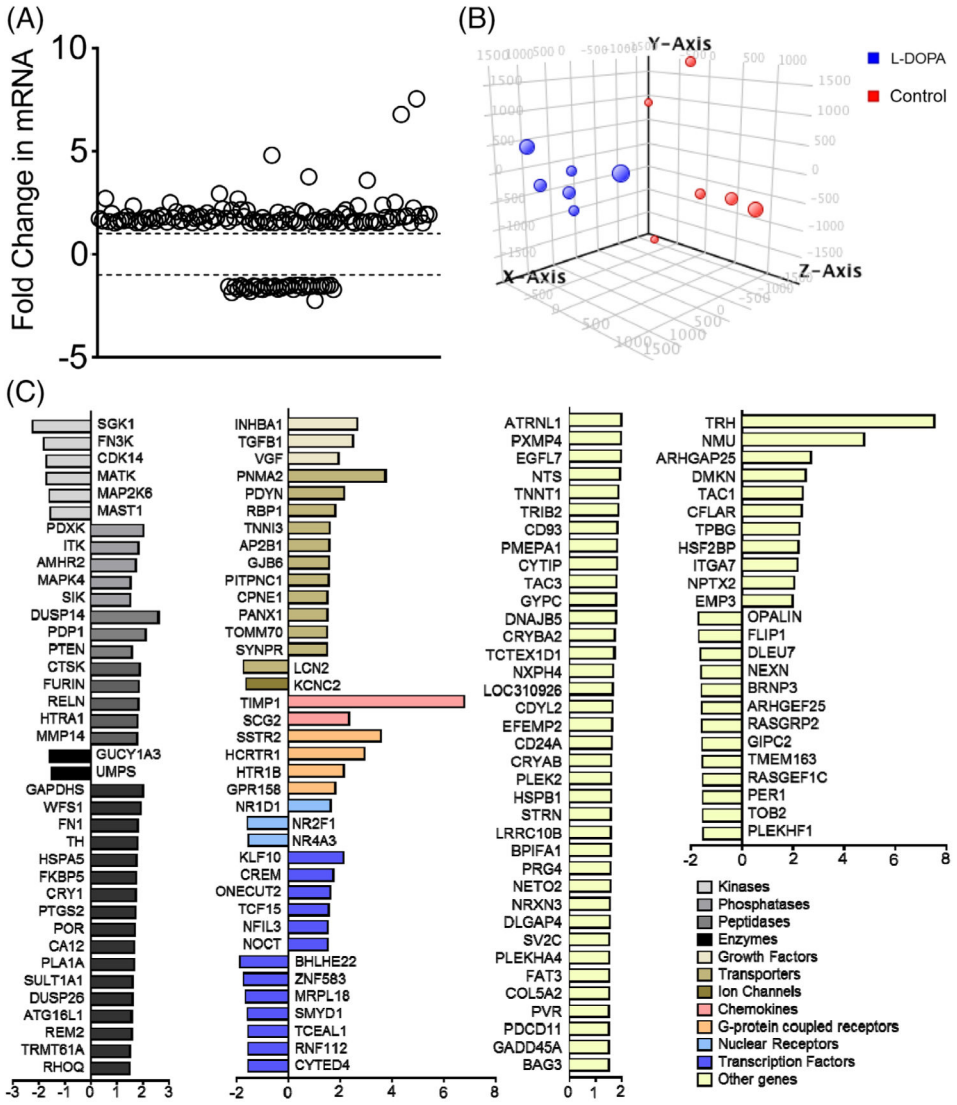

FIGURE 2.

Regulated genes identified in the striatum of parkinsonian rats following chronic L-Dopa treatment and development of long-term L-Dopa. A, Differentially regulated genes (1.5 FC and 0.05 *P*) that were identified in the striatum of L-Dopa-treated rats with unilateral 6-hydroxydopamine hydrobromide (6-OHDA) lesion of the nigrostriatal pathway depicted as fold change compared with control saline-treated rats (n = 6 each group) using microarray analysis of extracted mRNA (Materials and Methods). Fold change baseline was set to +1 for upregulated genes and −1 for downregulated genes. B, Principal component analysis (PCA) on transcriptomes of L-Dopa-treated rats (blue spots) and control saline-treated rats (red spots). Each spot indicates the location of a single animal in PCA plot based on its distinction in transcriptomic profile from other samples. C, Categories of genes differentially regulated in the striatum of L-Dopa-treated rats compared with control saline-treated rats (n = 6 each group). Differentially expressed genes (1.5 FC; 0.05 *P*) identified in microarray analysis were classified based on their product function using the IPA software

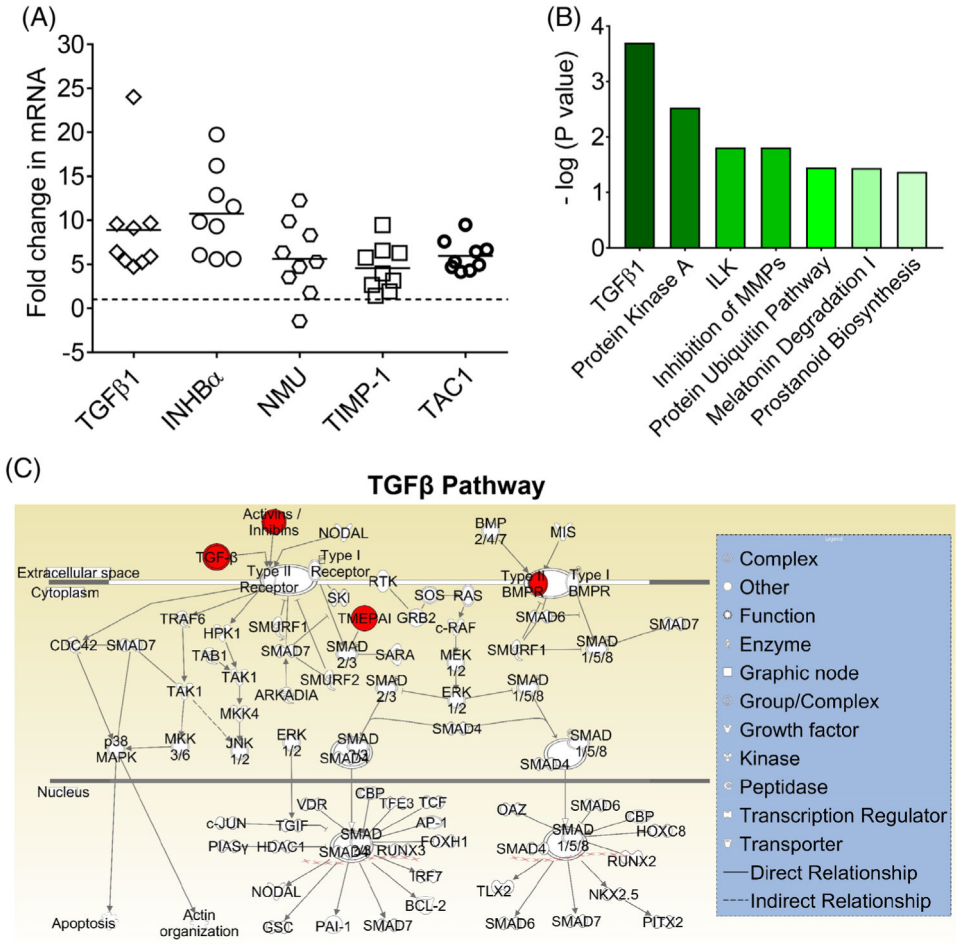

FIGURE 3.

Reverse transcription polymerase chain reaction (RT-PCR) analysis of upregulated genes and activated biological pathways in the striatum of L-Dopa-treated parkinsonian rats. A, *INHBA, TGFβ1, NMU, TIMP1* and *TAC1* mRNA expression was significantly higher in the striatum of L-Dopa-treated parkinsonian rats compared with control saline-treated rats (fold change vs average mRNA expression in saline-treated rats). The mRNA expression of each animal was normalized to *GAPDH* internal control as described in Materials and Methods. Significance was taken at a minimum of 1.5 fold change in L-Dopa-treated group of parkinsonian rats compared with control saline-treated rats (n = 6 each group). B, Pathways significantly upregulated (0.05 *P*) in L-Dopa-treated parkinsonian rats compared with controls (n = 6 each group) were identified by pathway enrichment tool using the IPA software based on the list of upregulated genes (>1.5 FC and 0.05 *P*). C, *TGFβ1* pathway is a top regulatory pathway in the striatum of L-Dopa-treated rats as identified in pathway enrichment analysis in the IPA software. Upregulated genes in *TGFβ1* pathway are indicated in red

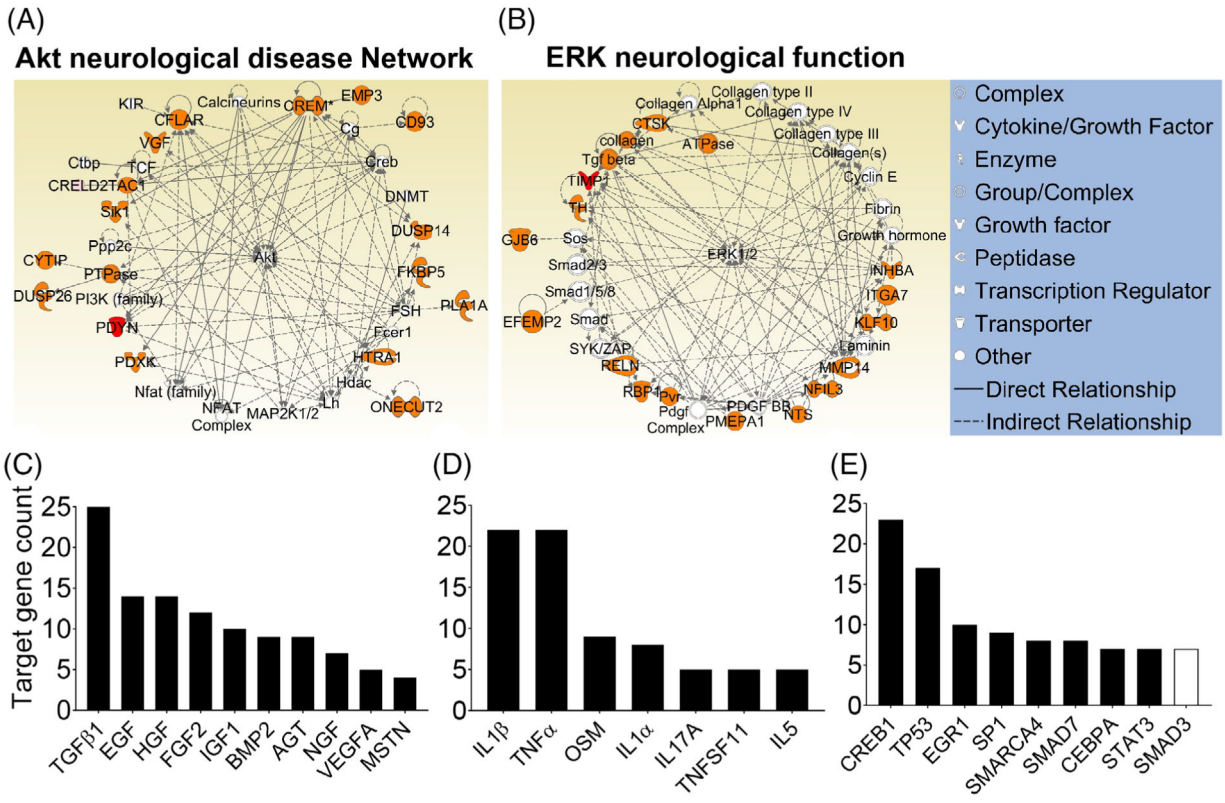

FIGURE 4.

Operated gene networks and upstream regulatory genes that may control the expression of upregulated genes in the striatum of L-Dopa-treated parkinsonian group of rats. A, *AKT* and B, *ERK*- (right) centered networks are regulated as predicted by significantly upregulated target genes in the striatum of L-Dopa-treated parkinsonian rats using gene networking analysis (IPA). Red color indicates transcript-upregulation. C, Growth factors; D, Cytokines; and E, Transcription factors to be modulated based on their targets from the list of differentially regulated genes (>1.5 FC and < 0.05 *P* value) in L-Dopa-treated compared with control saline-treated parkinsonian rats (Z score > 2.0 and 0.01 *P* value) using upstream regulator analysis tool in the IPA software. The counts of target genes are shown for each cytokine, growth factor and transcription factor on Y-axis

TABLE 1

List of pathways significantly induced (< 0.01 *P* value and 0.01 ratio) based on the involvement of upregulated genes (< 0.05 *P* value and 1.5-fold change) in L-Dopa-treated rats compared with control saline-treated rats (n = 6 each group)

Pathway	*P* value	Ratio	Genes
TGFβ signaling	0.0008	0.046	TGFβ1, INHBA, AMHR2, PMEPA1
Protein kinase A signaling	0.002	0.017	TH, DUSP26, TGFβ1, CREM, TNNI3, PTGS2, PTEN
ILK signaling	0.015	0.020	FN1, RHOQ, PTGS2, PTEN
Inhibition of MMPs	0.015	0.051	TIMP1, MMP14
Protein ubiquitination	0.035	0.015	CRYAB, HSPA5, DNAJB5, HSPB1
Melatonin degradation-I	0.036	0.032	POR, SULT1A1
Prostanoid biosynthesis	0.042	0.11	PTGS2